Mechanics of Advanced Composite Structures 10 (2023) 221 – 232

Semnan University

Mechanics of Advanced Composite Structures

journal homepage: http://MACS.journals.semnan.ac.ir

Longitudinal Vibration of Nanobeams by Two-Phase Local/Nonlocal Elasticity, Rayleigh Theory, and Generalized Differential Quadrature Method

R. Nazemnezhad *, R. Ashrafian

School of Engineering, Damghan University, Damghan, Iran

KEYWORDS

Longitudinal Vibration;
Nanobeam;
Two-Phase Elasticity.

ABSTRACT

To solve a differential equation of motion via more reliable procedures, it is essential to realize their efficiency. Whether Rayleigh's theory can be a compatible platform with two-phase local/nonlocal elasticity to render more reliable results compared to other theories or not is the main question that will be answered by this paper. Thus, nanobeam modeled by Rayleigh beam theory is analyzed by two-phase local/nonlocal elasticity. Governing equation in presence of the axial and transverse displacements is derived by means of Hamilton's principle and differential law of two-phase elasticity. Next, fourth-order Generalized Differential Quadrature Method (GDQM) is utilized to attain the discretized two-phase formulation. In order to confirm, the method and the results are compared with the exact solution prepared and presented in the literature. Moreover, the effects of various parameters such as geometrical properties like thickness, mode shape number, Local phase fraction coefficient, and nonlocal factor on the natural frequency are investigated to clarify that utilizing these theories with a common goal how ends with more accurate results, and how affects the natural frequencies.

1. Introduction

Focus on analyzing the natural behavior of nanoscale systems have been became one of the most crucial fields of study. The mechanical behavior of nanostructures enjoys vital importance due to their applications in nanodevices, such as nanomechanical resonators, nanoscale mass sensors, electromechanical nanoactuators, and nanogenerators. For instance, resonant frequencies are vastly vital in nanosensors to detect the type of viruses and bacteria. Theoretical results having relied on classical continuum theories have always been more convenient in contrast to other methods. Thus, new definitions or modifications of preliminary theories including strain gradient theory, nonlocal elastic theory, nonlocal strain gradient theory, and couple stress theory have been considered by numerous researchers. Some literature associated with the above-mentioned theories is eventually cited [1-7]. Farajpour et al. [8] in a review paper discussed two modified continuum-based theories, the nonlocal elasticity, and the nonlocal strain gradient elasticity employed to estimate the mechanical behavior of nanostructures. In that review paper, first, these two modified elasticity theories are briefly explained. Then, the nonlocal motion equations for different nanostructures including nanorods, nanorings, nanobeams, nanoplates, and nanoshells are derived. Defined stress in nonlocal theories is a dependent variable on the whole strain domain. Eringen by an integral formula based on the definition presented a simplified and constructive theory [4].

The simplicity of the differential form of Eringen's nonlocal elastic theory has attracted more interest to analyze mechanical problems. Furthermore, the hybrid of the differential form of this theory and strain gradient theory have both nonlocal and strain gradient effects. To enjoy further perception, more comprehensive studies are added [9-13]. The result in the mechanics of nanostructures studied by differential nonlocal shows that nonlocal parameter surging leads to a more softening effect. Although, the differential form of nonlocal

* Corresponding author. Tel.: +98-23-35220414
E-mail address: rnazemnezhad@du.ac.ir

DOI: 10.22075/macs.2023.25701.1374
Received 2021-12-26; Received in revised form 2022-12-26; Accepted 2023-01-01.

elasticity enjoys some paradoxical influences. Challamel et al. [14] in a paper, investigated the self-adjointness of Eringen's nonlocal elasticity based on simple one-dimensional beam models. It was shown that Eringen's model may be nonself-adjoint and that it can result in an unexpected stiffening effect for a cantilever's fundamental vibration frequency with respect to increasing Eringen's small length scale coefficient. Fernandez-Saez et al. [15] formulated the problem of the static bending of Euler–Bernoulli beams using the Eringen integral constitutive equation. Beams with different boundary and load conditions are analyzed and the results are compared with those derived from the differential approach showing that they are different in general. Appuzo et al. [16] investigated free vibrations of nano-beams by making recourse to the novel stress-driven nonlocal integral model (SDM). Natural frequencies evaluated according to the SDM are compared with those obtained by the Eringen differential law (EDM) and by the gradient elasticity theory (GradEla). SDM provides an effective methodology to describe nonlocal phenomena. To enjoy a more constructive method, Eringen's combination of local and nonlocal has been used by researchers, for example, Wang et al. [17] analyzed static bending of nonlocal Euler-Bernoulli beams using Eringen's two-phase local/nonlocal model by an analytical study. Additionally, it was stated that the controversial nonlocal beam problem in the literature is well resolved by the reduction method, and Zhu et al. [18] adopted Eringen's two-phase nonlocal integral model to carry out an analytical study on the buckling problem of Euler-Bernoulli beams by using a reduction method. Qing [19] combined strain and strain-driven two-phase nonlocal integral polar models to model the axisymmetric bending of circular microplates. The results showed that the purely strain-driven nonlocal integral polar model turns to a traditional nonlocal differential polar model if the constitutive constraints are neglected. Khaniki [20] stated that the differential form of Eringen's nonlocal elastic theory has some inaccuracies in analyzing small-scale structures with different boundary conditions. Accordingly, in this work, a comprehensive study on the vibration behavior of double-layered nanobeam systems (DNBS) was presented within the framework of Eringen's two-phase local/nonlocal integral mode. Fakher, and Hosseini-Hashemi [21] through the exact solution corresponding to the vibrations of two-phase Timoshenko nanobeams provided the shear-locking problem investigated in the case of the two-phase finite element method (FEM). Moreover, since the FE model of local/nonlocal nanobeam is more complex than the classic one, due to the coupling of all elements together, they created an efficient locking-free local/nonlocal FEM with a simple and efficient beam element. Employing nonlocal models with classical boundary conditions may lead to inconsistency. Thus, higher-order boundary conditions along with two-phase differential equations can render the most accurate results compared with conventional patterns. Shaat et al. [22] formed consistent boundary conditions by iterative nonlocal residual approach. This approach solves the field equation in the local field with an imposed nonlocal residual. Rayleigh theory's displacement field, which its simple form has been employed vastly thus far unlike this form utilized in this study for the first time, and two-phase local/nonlocal elasticity are utilized to analyze the longitudinal vibration of nanobeams. Governing equations, in presence of the axial and transverse displacements, are derived by means of Hamilton's principle and differential law of two-phase elasticity. To solve numerically, the Generalized Differential Quadrature Method (GDQM) is utilized to attain the discretized two-phase formulation. Eventually a verification, and the result are prepared. Also, the effects of various parameters such as, geometrical properties, nonlocal parameters, and local phase fraction coefficient on the natural frequencies are investigated. The unique feature of the present work is the effective use of two-phase elasticity theory in modeling the longitudinal vibrations of nanobeams and the use of appropriate solution methods in the field of related differential equations, which has eliminated the contradictions compared to the common non-local differential theory. Also, the softening effect of non-local parameters appears more strongly in the two-phase domain.

2. Problem Formulation

The equation of motion and boundary conditions of Rayleigh nanobeams are obtained as the first step. The geometry and coordinates of the nanobeam model, and displacement fields, according to the Rayleigh beam theory, are assumed as follows.

$$\begin{aligned} U &= u(x,t) \\ V &= -vy\frac{\partial u(x,t)}{\partial x} \\ W &= -vz\frac{\partial u(x,t)}{\partial x} \\ \varepsilon_{xx} &= \frac{\partial U}{\partial x} \\ \varepsilon_{yy} &= \varepsilon_{zz} = 0 \\ \varepsilon_{xy} &= \varepsilon_{zx} = \varepsilon_{yz} = 0 \end{aligned} \tag{1}$$

ν shows Poisson's ratio in Eq.1. In this theory, the inertia of the lateral motions by which the cross sections are extended or contracted in their planes is considered. But the contribution of shear stiffness to the strain energy is neglected. An element in the cross-section of the beam, located at the coordinates y and z, undergoes the lateral displacement $-\nu y\, \partial u(x,t)/\partial x$ and $-\nu z\, \partial u(x,t)/\partial x$, respectively along the y and z directions. Nanobeam strain energy is [23]

$$\pi = \frac{1}{2}\iiint_{Vo} (\sigma_{xx}\varepsilon_{xx})dV \tag{2}$$

Axial force, $N(x,t) = \int_A \sigma_{xx} dA$, should be defined and by using Eq. (1), Eq. (2) is rewritten as

$$\pi = \frac{1}{2}\int_0^L \left(N(x,t)\left(\frac{\partial U}{\partial x}\right)\right)dx \tag{3}$$

The kinetic energy of the beam can be obtained as

$$T = \frac{1}{2}\int_0^L dx \int_0^A \rho dA\,[\left(\frac{\partial U}{\partial t}\right)^2 + \left(\frac{\partial V}{\partial t}\right)^2 + \left(\frac{\partial W}{\partial t}\right)^2] \tag{4}$$

After simplification, the kinetic energy enjoys the shape below, thus

$$T = \frac{1}{2}\int_0^L \rho A\left(\frac{\partial U}{\partial t}\right)^2 dx + \frac{1}{2}\int_0^L \rho \nu^2 I_p \left(\frac{\partial^2 U}{\partial x \partial t}\right)^2 dx \tag{5}$$

where ρ is the material density, and I_p is defined by

$$I_p = \int_A (y^2 + z^2)dA \tag{6}$$

In the following, governing equations and boundary conditions will be obtained by employing Hamilton's principle.

$$\delta \int_{t_1}^{t_2} (T - \pi + W)\, dt = 0 \tag{7}$$

According to Eqs. (3) and (5), variations of the potential and kinetic energies are presented.

$$\int_{t_1}^{t_2} \delta\pi dt = \int_{t_1}^{t_2} (N(x,t)\delta u(x,t)|_0^L - \int_0^L \frac{\partial N(x,t)}{\partial x}\delta u(x,t)dx)dt \tag{8}$$

$$\int_{t_1}^{t_2} \delta T dt = - \int_0^L \int_{t_1}^{t_2} \rho A \delta u(x,t)\left(\frac{\partial^2 u(x,t)}{\partial t^2}\right)dtdx - \int_{t_1}^{t_2} \rho \nu^2 I_p (\frac{\partial^3 u(x,t)}{\partial x \partial t^2}\delta u(x,t)|_0^L + \int_0^l \delta u(x,t)\left(\frac{\partial}{\partial x}\right)\left(\frac{\partial^3 u(x,t)}{\partial x \partial t^2}\right)dx)dt$$

In this step, by substituting Eq. (8) into Eq. (7), the governing equation can be obtained.

$$\frac{\partial N(x,t)}{\partial x} - \rho A\left(\frac{\partial^2 u}{\partial t^2}\right) + \rho \nu^2 I_p \left(\frac{\partial^4 u}{\partial x^2 \partial t^2}\right) = 0 \tag{9}$$

Also, corresponding boundary conditions of that are expressed as

$$(N(x,t) + \rho \nu^2 I_p \left(\frac{\partial}{\partial x}\right)\left(\frac{\partial^3 u}{\partial x \partial t^2}\right))\delta u|_0^L = 0 \tag{10}$$

Note that Eq. (10) is satisfied if the beam is either fixed or free at the ends $x = 0$ and $x = L$. At a fixed end, $u = 0$ and hence $\delta u = 0$, while

$$N(x,t) + \rho \nu^2 I_p \left(\frac{\partial}{\partial x}\right)\left(\frac{\partial^3 u}{\partial x \partial t^2}\right) = 0 \tag{11}$$

at a free end [23].

3. Two Phase Elasticity

Two-phase local/nonlocal elasticity is shown below comprising local and nonlocal parts.

$$t(x) = \zeta \bar{C}: \varepsilon(x) + (1-\xi)\int_{\bar{V}} \alpha(x,\bar{x},\kappa)\, \bar{C}: \varepsilon(\bar{x})d\bar{V} \tag{12}$$

$$\alpha(x,\bar{x},\kappa) = \frac{1}{2\kappa} e^{-\frac{|x-\bar{x}|}{\kappa}} \tag{13}$$

The definition of the parameters employed in this study is listed in the nomenclature. Reference [24] presented the equal differential of the integral equation with two constitutive boundary conditions (CBC) as follows.

$$G(x) = Y(x) + C\int_a^b e^{\mu|x-\bar{x}|}\, Y(\bar{x})d\bar{x} \tag{14}$$

$$\ddot{Y}(x) + \mu(2\mathrm{C} - \mu)Y(x) = \ddot{G}(x) - \mu^2 G(x) \tag{15}$$

$$\dot{Y}(a) + \mu Y(a) = \dot{G}(a) + \mu G(a) \tag{16}$$

$$\dot{Y}(b) - \mu Y(b) = \dot{G}(b) - \mu G(b) \tag{17}$$

Eq. (15) is a differential form of Eq. (14), and two additional boundary conditions are essential to be satisfied.

4. Two-Phase Axial Force

By using the Eqs. (12), (13) and the primary form of axial force defined earlier, the two-phase axial force is written as

$$\begin{aligned} &N(x,t) \\ &= \zeta EA\frac{\partial u(x,t)}{\partial x} \\ &+ EA\frac{(1-\zeta)}{2\kappa}\int_0^L e^{-\frac{|x-\bar{x}|}{\kappa}}\left(\frac{\partial u(\bar{x},t)}{\partial \bar{x}}\right)d\bar{x} \end{aligned} \tag{18}$$

E is the elastic modulus, and A is the cross-section of the nanobeam. Now, by employing Eqs. (14), (15), and (18) as well as a governing equation, the differential form of axial force is derived as below.

$$\begin{aligned} N(x,t) = &-\rho v^2 I_p \kappa^2\left(\frac{\partial^5 u(x,t)}{\partial x^3 \partial t^2}\right) \\ &+ \rho A\kappa^2\left(\frac{\partial^3 u(x,t)}{\partial x \partial t^2}\right) \\ &+ EA\left(\frac{\partial u(x,t)}{\partial x}\right) \\ &- \zeta EA\kappa^2\frac{\partial^3 u(x,t)}{\partial x^3} \end{aligned} \tag{19}$$

Eventually, by substituting Eq. (19) into governing equation, the expected form of governing equation is derived.

$$\begin{aligned} &(-\rho v^2 I_p \kappa^2\left(\frac{\partial^4 u(x,t)}{\partial x^4}\right) + (\rho A\kappa^2 \\ &\quad + \rho v^2 I_p)\left(\frac{\partial^2 u(x,t)}{\partial x^2}\right) \\ &\quad - \rho A)\left(\frac{\partial^2 u(x,t)}{\partial t^2}\right) \\ &\quad = \zeta EA\kappa^2\left(\frac{\partial^4 u(x,t)}{\partial x^4}\right) \\ &\quad - EA\left(\frac{\partial^2 u(x,t)}{\partial x^2}\right) \end{aligned} \tag{20}$$

And, according to Eqs. (16), (17), and (19) the CBCs of axial force will be obtained as

$$\begin{aligned} &\zeta EA\kappa^2\left(\frac{\partial^4 u(x,t)}{\partial x^4}\right) - \zeta EA\kappa\left(\frac{\partial^3 u(x,t)}{\partial x^3}\right) \\ &- EA\left(\frac{\partial^2 u(x,t)}{\partial x^2}\right)(1-\zeta) \\ &- \frac{EA}{\kappa}\left(\frac{\partial u(x,t)}{\partial x}\right)(\zeta+1) \\ &= \left(-\rho v^2 I_p \kappa^2\left(\frac{\partial^4 u(x,t)}{\partial x^4}\right)\right. \\ &+ \rho A\kappa^2\left(\frac{\partial^2 u(x,t)}{\partial x^2}\right) + \rho v^2 I_p \kappa\left(\frac{\partial^3 u(x,t)}{\partial x^3}\right) \\ &\left.- \rho A\kappa\left(\frac{\partial u(x,t)}{\partial x}\right)\right)\left(\frac{\partial^2 u(x,t)}{\partial t^2}\right) \; at\; x = 0 \end{aligned} \tag{21}$$

$$\begin{aligned} &\zeta EA\kappa^2\left(\frac{\partial^4 u(x,t)}{\partial x^4}\right) + \zeta EA\kappa\left(\frac{\partial^3 u(x,t)}{\partial x^3}\right) \\ &+ EA\left(\frac{\partial^2 u(x,t)}{\partial x^2}\right)(\zeta-1) \\ &- \frac{EA}{\kappa}\left(\frac{\partial u(x,t)}{\partial x}\right)(1-\zeta) \\ &= \left(-\rho v^2 I_p \kappa^2\left(\frac{\partial^4 u(x,t)}{\partial x^4}\right)\right. \\ &+ \rho A\kappa^2\left(\frac{\partial^2 u(x,t)}{\partial x^2}\right) - \rho v^2 I_p \kappa\left(\frac{\partial^3 u(x,t)}{\partial x^3}\right) \\ &\left.+ \rho A\kappa\left(\frac{\partial u(x,t)}{\partial x}\right)\right)\left(\frac{\partial^2 u(x,t)}{\partial t^2}\right) \; at\; x = L \end{aligned} \tag{22}$$

5. Generalized Differential Quadrature Method (GDQM)

Amid other numerical means such as the Galerkin method and finite element method, the GDQM has numerous beneficial attributes, that is, simple mathematical principle, the high pace of convergence, high accuracy, small calculation amount, and less memory demand, etc. The generalized differential quadrature method (GDQM) has been proposed as a general numerical method to solve high-order differential equations. Based on the fourth-order derivatives GDQM, the r-th order derivative of a function is considered as follows

$$\begin{aligned} \Psi^{(r)}(x_i) = &\sum_{j=1}^{ns} h_{j0}^{(r)}(x_i)\Psi_j + h_{11}^{(r)}(x_i)\Psi_1^{(1)} \\ &+ h_{ns1}^{(r)}(x_i)\Psi_{ns}^{(1)} \\ &= \sum_{j=1}^{ns+2}\beta_{ij}^{(r)} V_j \quad i \\ &= 1,2,\dots,ns \end{aligned} \tag{23}$$

Hermite shape functions are as follows

$$\beta_{ijl}^{(r)} = h_{jl}^{(r)}(x_i) = \frac{d^r h_{jl}(x_i)}{dx^r} \tag{24}$$

$$h_{jl}^{(r)}(x_i) = \begin{cases} 1 & if\ i = j\ \&\ l = r \\ 0 & otherwise \end{cases} \tag{25}$$

$$\begin{aligned} h_{pi}(x) = &\left(a_{pi}x^2 + b_{pi}x + c_{pi}\right)l_p(x) \quad p \\ &= 1, ns\ and\ i = 0,1 \end{aligned} \tag{26}$$

$$\begin{aligned} h_{j0}(x) = &\frac{(x-x_1)(x-x_{ns})}{(x_j-x_1)(x_j-x_{ns})}l_j(x) \quad j \\ &= 2,3,\dots,ns-1 \end{aligned} \tag{27}$$

where a_{pi}, b_{pi}, and c_{pi} are given in appendix-I. Also, $l_j(x)$ is equivalent to the δ_{ij}. Also, the weighting coefficients, Lagrangian interpolation for the first derivative, and higher-order derivatives can be expressed as

$$l_j^{(1)}(x_i) = \begin{cases} \dfrac{R^{(1)}(x_i)}{(x_i - x_j)R^{(1)}(x_j)} & i,j = 1,2,\dots,ns; i \neq j \\ -\sum\limits_{j=1,\ i\neq j}^{ns} l_j^{(1)}(x_i) & i,j = 1,2,\dots,ns \end{cases} \quad (28)$$

$$R^{(1)}(x_i) = \prod_{m=1,\ m\neq i}^{ns} (x_i - x_m) \quad (29)$$

$$l_j^{(r)}(x_i) = \begin{cases} r(l_i^{(r-1)}(x_i) l_j^{(1)}(x_i) - \dfrac{l_j^{(r-1)}(x_i)}{(x_i - x_j)}) & i,j = 1,2,\dots,ns; i \neq j \\ -\sum\limits_{j=1,\ i\neq j}^{ns} l_j^{(r)}(x_i) & i,j = 1,2,\dots,ns \end{cases} \quad (30)$$

Both the equal space model and Chebyshev Gauss Lobatto model could be used, however owing to further reliable and quick convergence, the latter, that is eq. (32), is utilized. Also, the discretized form of the function could be defined as follows

$$\{V\}^T = \left\{\Psi_1^{(0)}, \Psi_1^{(1)}, \Psi_2, \Psi_3, \dots, \Psi_{ns-1}, \Psi_{ns}^{(0)}, \Psi_{ns}^{(1)}\right\} = \{V_1, V_2, \dots, V_{ns+2}\} \quad (31)$$

$$x_i = \frac{L}{2}\left[1 - \cos\left(\frac{(i-1)}{(ns-1)}\pi\right)\right] \qquad i = 1,2,\dots,ns \quad (32)$$

6. Vibration Analysis

To analyze the vibrational status of the system, harmonic vibration has been assumed, thus the displacement field can be shaped as shown below

$$U(x,t) = U(x)e^{i\lambda t} \quad (33)$$

$$\{U\}^T = \{U_1, U_2, \dots, U_{ns+2}\}^T \quad (34)$$

To derive the discretized governing equations in the axial direction by utilizing Eqs. (33) and (34) into Eqs. (20), can be the final segment to achieve expected results.

$$\left(-\rho\nu^2 I_p\kappa^2 \sum_{j=1}^{ns+2} \beta_{ij}^{(4)} U_j + \left(\rho A\kappa^2 + \rho\nu^2 I_p\right) \sum_{j=1}^{ns+2} \beta_{ij}^{(2)} U_j - \rho A U_{i+1}\right)(-\lambda^2) = \zeta EA\kappa^2 \sum_{j=1}^{ns+2} \beta_{ij}^{(4)} U_j - EA \sum_{j=1}^{ns+2} \beta_{ij}^{(2)} U_j \quad (35)$$

Furthermore, applying Eqs. (33) and (34) into Eqs. (21), and (22) finalize the discrete type of CBCs. The matrix, shown below, comprising a discrete governing equation and all of the boundary conditions shows that solving such an eigenvalue problem ends to the natural frequencies and corresponding mode shapes.

$$\begin{aligned} &\zeta EA\kappa^2 \sum_{j=1}^{ns+2} \beta_{ij}^{(4)} U_j - \zeta EA\kappa \sum_{j=1}^{ns+2} \beta_{ij}^{(3)} U_j \\ &-EA(1-\zeta) \sum_{j=1}^{ns+2} \beta_{ij}^{(2)} U_j - \frac{EA}{\kappa}(\zeta+1)U_2 \\ &= \left(-\rho\nu^2 I_p\kappa^2 \sum_{j=1}^{ns+2} \beta_{ij}^{(4)} U_j + \rho A\kappa^2 \sum_{j=1}^{ns+2} \beta_{ij}^{(2)} U_j + \rho\nu^2 I_p\kappa \sum_{j=1}^{ns+2} \beta_{ij}^{(3)} U_j - \rho A\kappa U_2\right)(-\lambda^2) \quad at\ x = 0 \end{aligned} \quad (36)$$

$$\begin{aligned} &\zeta EA\kappa^2 \sum_{j=1}^{ns+2} \beta_{ij}^{(4)} U_j + \zeta EA\kappa \sum_{j=1}^{ns+2} \beta_{ij}^{(3)} U_j \\ &+EA(\zeta-1) \sum_{j=1}^{ns+2} \beta_{ij}^{(2)} U_j - \frac{EA}{\kappa}(1-\zeta)U_{ns+2} \\ &= \left(-\rho\nu^2 I_p\kappa^2 \sum_{j=1}^{ns+2} \beta_{ij}^{(4)} U_j + \rho A\kappa^2 \sum_{j=1}^{ns+2} \beta_{ij}^{(2)} U_j - \rho\nu^2 I_p\kappa \sum_{j=1}^{ns+2} \beta_{ij}^{(3)} U_j + \rho A\kappa U_{ns+2}\right)(-\lambda^2) \quad at\ x = L \end{aligned} \quad (37)$$

$$\begin{bmatrix} [K_{bb}]_{4*4} & [K_{bd}]_{4*(ns-2)} \\ [K_{db}]_{(ns-2)*4} & [K_{dd}]_{(ns-2)*(ns-2)} \end{bmatrix} \begin{Bmatrix} \{V_b\} \\ \{V_d\} \end{Bmatrix} - \lambda^2 \begin{bmatrix} [M_{bb}]_{4*4} & [M_{bd}]_{4*(ns-2)} \\ [M_{db}]_{(ns-2)*4} & [M_{dd}]_{(ns-2)*(ns-2)} \end{bmatrix} \begin{Bmatrix} \{V_b\} \\ \{V_d\} \end{Bmatrix} = 0 \quad (38)$$

7. Numerical Results

To realize the influences of axial displacements on the vibration of a nanosensor, corresponding results are extracted and presented in three portions. The first is devoted to the verification of the employed method, and the other two portions presented the numerical achievements of this work. In all results, the material listed below in Table.1 is utilized.

Table 1. Material Properties

Material Properties	
ρ	1000 (kg/m^3)
ν	0.3
κ/L	0.1~0.5
h/L	0.05~0.1
E	1.44e9 (GPa)
L	2 (nm)

In the first portion, the whole derivation process of formulas has been carried on by assuming $\zeta = 1$. Thus, the employed theory became fully local, and the assumption made it possible to enjoy sufficient verification compared with the essential natural frequency formula obtained by Rao. [23]. The formula is indexed below for further assessment.

$$\omega_n^2 = \frac{n^2\pi^2}{\left(1 + \nu^2 n^2 \pi^2 I_p / AL^2\right)} \frac{E}{\rho l^2} \tag{39}$$

Figures 1 and 2 comprising the first and second five natural frequencies, and their exact targets towards which curves converge show the path of progress of GDQM. For the first and second natural frequencies, there is a similar pattern, that is, on nearly 23 sample points, a sharp decline occurs, and they approach the exact solution. For the rest of the natural frequencies, various statuses should be considered. The rash decrease happened on almost 51 sample points. As expected, increasing the number of sample points cause further convergence and precise results. Overall, it can be obviously seen that it is possible to achieve the desired accuracy by utilizing 150 sample points. To enjoy the higher quality, the horizontal axis of the above-mentioned figures is divided into 100.

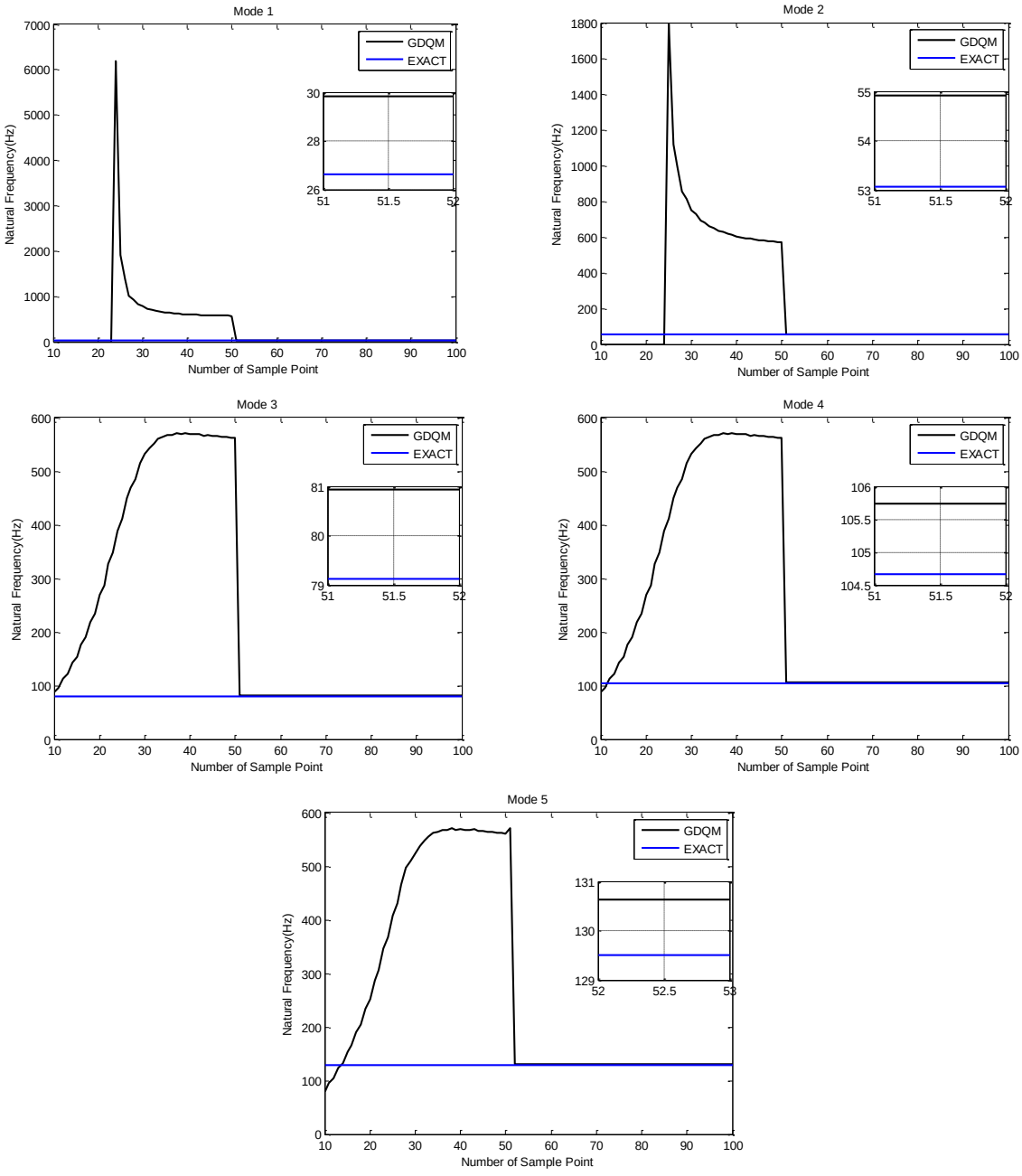

Fig. 1. First five natural frequencies with $\zeta = 1$

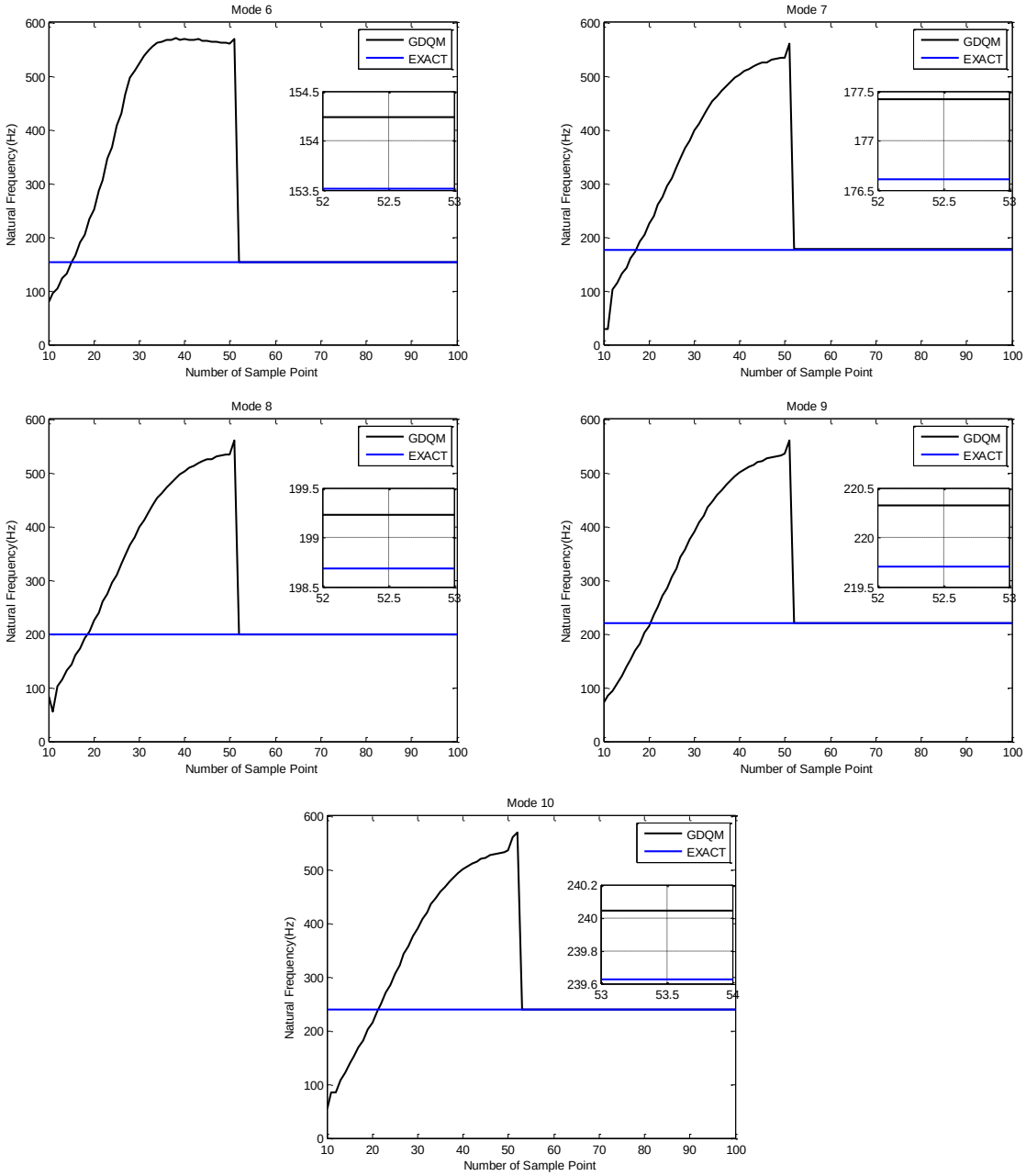

Fig. 2. Second five natural frequencies with $\zeta = 1$

Figure 3 deals with generating an amplitude of the local phase fraction coefficient, and truly shows the 10 variants of natural frequencies, and how it changes along the horizontal axis or distinct ζ. Figure 3 is presented the first ten natural frequencies. There, the first natural frequency experiences a sharp fluctuation which occurs almost in intervals 0∼0.05. Then, it begins a stable climbing, however, the slope compared with other variants is considerable. What is essential to state here is that 0∼0.05 interval is a region on which investigation does not result in a particular consequence, and with increasing local phase fraction coefficient, the order and natural frequencies raised in a hugely noticeable way. Thus, it can be stated that zeta parameter enjoys a vastly crucial role in final quantities.

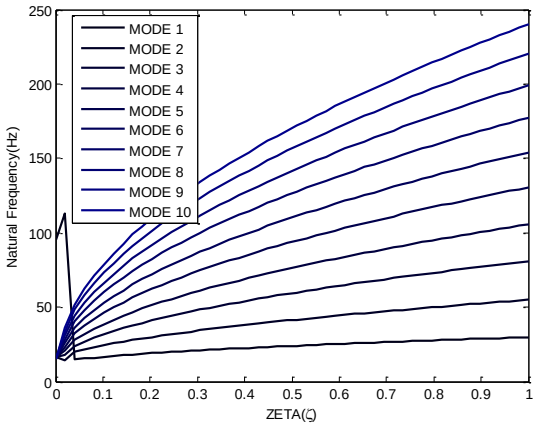

Fig. 3. Natural Frequencies with Zeta amplitude

Table 2. demonstrates the trend of the first 5 natural frequencies with regard to distinct values

of thickness and local phase fraction coefficient. Three and five independent values for the two above-mentioned variables are defined. It is obvious that increasing h/L leads to an inconsiderable decline of natural frequencies. The decline for upper cases of natural frequency can be severe, and further. Additionally, this type of trend of natural frequency can be seen for the distinct value of the local phase fraction coefficient. What is mentionable in the next table, Table 3., is the demonstration of the relation of natural frequencies with nonlocal factors and local phase fraction coefficient that is not as clear as in the prior section. It can be stated that zeta 0.2, 0.4, and 0.6 for all quantities of κ/L enjoy similar effects on natural frequency in comparison with the previous table showed, but the two last cases of local phase fraction coefficient show a completely different approach. For 0.8 all differences are intensively low, and for 1, the behavior is predictable. In other words, the nonlocal factor is constructive in the process while the local phase fraction coefficient does not reach the ultimate value.

Table 2. The first five Natural Frequencies with various h and ζ

ζ	h/L	Mode Number				
		1st	2nd	3rd	4th	5th
0.2	0.05	18.9959	29.8722	41.1043	51.5548	63.0791
	0.075	18.9854	29.8237	40.9603	51.2477	62.4990
	0.1	18.9716	29.7570	40.7590	50.8256	61.7135
0.4	0.05	22.5631	38.0495	54.3944	69.8905	86.3596
	0.075	22.5376	38.0009	54.2133	69.4787	85.5764
	0.1	22.5248	37.9215	53.9563	68.9165	84.5165
0.6	0.05	25.3353	44.5360	64.7942	84.2136	104.4723
	0.075	25.3189	44.4761	64.5753	83.7217	103.5302
	0.1	25.3050	44.3839	64.2751	83.0470	102.2484
0.8	0.05	27.7061	50.1253	73.6769	96.4056	119.8565
	0.075	27.6992	50.0518	73.4260	95.8436	118.7762
	0.1	27.6870	49.9420	73.0924	95.0704	117.3090
1	0.05	29.8637	55.0860	81.5789	107.2133	133.4731
	0.075	29.8328	55.0240	81.3025	106.5870	132.2703
	0.1	29.8103	54.9187	80.9242	105.7299	130.6347

Table 3. The first five Natural |Frequencies with various K and ζ

ζ	κ/L	Mode Number				
		1st	2nd	3rd	4th	5th
0.2	0.1	24.9743	46.1374	62.5482	75.3673	86.0071
	0.2	22.8861	38.6334	50.0314	60.1094	69.7962
	0.3	21.1401	34.1179	44.6697	54.7428	64.8907
	0.4	19.8690	31.4545	42.1386	52.2470	62.8104
	0.5	18.9716	29.7570	40.7590	50.8256	61.7135
0.4	0.1	25.8425	48.7280	68.0464	84.7580	99.8715
	0.2	24.6653	43.8405	59.9263	75.0148	89.6937
	0.3	23.7058	40.9163	56.5348	71.5662	86.5978
	0.4	23.0207	39.1188	54.8931	69.8924	85.2461
	0.5	22.5248	37.9215	53.9563	68.9165	84.5165
0.6	0.1	26.5934	51.0556	72.9800	93.0233	111.8100
	0.2	26.2108	48.2883	68.1394	87.1192	105.6250
	0.3	25.8533	46.4712	66.0084	84.8794	103.6405
	0.4	25.5592	45.2477	64.9206	83.7323	102.7439
	0.5	25.3050	44.3839	64.2751	83.0470	102.2484
0.8	0.1	27.2848	53.2243	77.5309	100.5206	122.4807
	0.2	27.6184	52.2618	75.3441	97.6204	119.3487
	0.3	27.7528	51.3164	74.1748	96.2959	118.1916
	0.4	27.7567	50.5421	73.5118	95.5462	117.6309
	0.5	27.6870	49.9420	73.0924	95.0704	117.3090
1	0.1	27.9381	55.2773	81.7886	107.4436	132.2327
	0.2	28.9256	55.8997	81.8592	107.0441	131.6063
	0.3	29.4801	55.6877	81.4785	106.4668	131.1149
	0.4	29.7353	55.2888	81.1658	106.0355	130.8222
	0.5	29.8103	54.9187	80.9242	105.7299	130.6347

8. Conclusion

Two-phase local/nonlocal elasticity as the essential theory is utilized to investigate the longitudinal vibration of Rayleigh nanobeams. The generalized differential quadrature method solves the differential equation of motion. Rayleigh's theory and two-phase local/nonlocal elasticity demonstrate a reliable linkage that ends with accessible results. In this study, results truly show that employing the main theories result in acceptable consequences. Nonlocal factors and local phase fraction coefficients may significantly decrease or increase the frequencies. The details were described in the prior section, but it can be mentioned that the geometrical parameters can enjoy a more significant effect on natural frequency than other mentioned parameters.

Moreover, the displayed discrepancy between distinct mode shapes and natural frequencies, in Fig. 3 with regard to the local phase fraction coefficient illustrates the importance of the employed independent variable. The compatibility of GDQM with vibration analysis of two-phase Rayleigh nanobeam is confirmed by comparison with an analytical procedure, even though considerable amounts of sample points were needed to attain. One of the main novelties of the current work is employing two-phase elasticity theory without contradiction in modelling longitudinal vibrations of nanobeams as well as the development of proper solution procedures in the domain of corresponding differential equations that in comparison with common nonlocal differential theory eliminated contradictions and consequently provides Integral form of results in accordance with differential one.

Moreover, by comparing the results of two-phase theory and nonlocal, it can be said that in addition to the elimination of contradictions softening effect of nonlocal parameter consideration appears with more intensity in the two-phase domain (with a quantity close to zero) that this enjoys more discrepancy in higher modes. Eventually, this is essentially considering that according to the complexity related to the manner of creation of atomic linkage between the nanostructure and supportive surfaces, utilizing classical boundary conditions in modelling nanostructures can make errors, thus employing higher order boundary conditions along with two-phase differential equations enjoys vital importance. Thus, it can be mentioned here that the development of models concerning boundary conditions is constructive to enhance the accuracy of prediction of mechanics of nanomachines, and more research in this field is needed.

Nomenclature

L	Length
b	Width
h	Thickness
U, V, W	Displacement fields
π	Strain energy
Vo	Volume of the nanobeam
σ_{xx}	Normal stress
ε_{xx}	Normal strain
N	Axial force
T	Kinetic energy
I_p	Polar moment of the inertia of the cross-section
$t(x)$	Stress in two-phase state
ζ	Local phase fraction coefficient
α	Kernel function
ε	Strain tensor
$\bar{C}$	Elasticity tensor
$\bar{V}$	Volume of the domain
κ	Nonlocal factor
$C\&\mu$	Constant coefficients.
ns	Number of sample points,
x_i	Location of sample points,
$h_{j0}^{(r)}$	Hermite shape functions for all sample points,
$h_{11}^{(r)}$	Hermite shape functions for Rth order derivative at the first sample point
$h_{ns1}^{(r)}$	Hermite shape functions for Rth order derivative at the last sample point
a_{pi}, b_{pi}, c_{pi}	Constant coefficients
$l_j(x)$	Lagrangian interpolation test functions
δ_{ij}	Kronecker delta
ν	Poisson's ratio
ρ	Density

Appendix I

$$\begin{cases} a_{10} = \dfrac{-1}{(x_1 - x_{ns})^2} + \dfrac{-l_1^{(1)}(x_1)}{(x_1 - x_{ns})} \\ b_{10} = \dfrac{1}{(x_1 - x_{ns})} - a_{10}(x_1 + x_{ns}) \\ c_{10} = 1 - a_{10}{x_1}^2 - b_{10}x_1 \end{cases}$$

$$\begin{cases} a_{11} = \dfrac{1}{x_1 - x_{ns}} \\ b_{11} = \dfrac{-(x_1 + x_{ns})}{x_1 - x_{ns}} \\ c_{11} = \dfrac{x_1 x_{ns}}{x_1 - x_{ns}} \end{cases}$$

$$\begin{cases} a_{ns0} = \dfrac{-1}{(x_1 - x_{ns})^2} + \dfrac{-l_{ns}^{(1)}(x_1)}{(x_1 - x_{ns})} \\ b_{ns0} = \dfrac{-1}{(x_1 - x_{ns})} - a_{ns0}(x_1 + x_{ns}) \\ c_{ns0} = 1 - a_{ns0}{x_{ns}}^2 - b_{ns0}x_{ns} \end{cases}$$

$$\begin{cases} a_{ns1} = \dfrac{-1}{x_1 - x_{ns}} \\ b_{ns1} = \dfrac{x_1 + x_{ns}}{x_1 - x_{ns}} \\ c_{ns1} = \dfrac{-x_1 x_{ns}}{x_1 - x_{ns}} \end{cases}$$

Appendix II

$$\int_{t_1}^{t_2} \delta T dt = \int_{t_1}^{t_2} \left(\int_0^L \rho A\, \delta\left(\frac{\partial u}{\partial t}\right)\left(\frac{\partial u}{\partial t}\right) dx + \int_0^L \rho v^2 I_p\, \delta\left(\frac{\partial^2 u}{\partial x \partial t}\right)^2 dx \right) dt$$

Transformation of Integral order, the first part

$$\gg \int_{t_1}^{t_2} \delta\left(\frac{\partial u}{\partial t}\right)\left(\frac{\partial u}{\partial t}\right) dt = \left(\frac{\partial u}{\partial t}\right)\delta u(x,t)\Big|_{t_1}^{t_2} - \int_{t_1}^{t_2} \delta u(x,t)\left(\frac{\partial^2 u}{\partial t^2}\right) dt$$

The Second part

$$\gg \int_{t_1}^{t_2} \delta\left(\frac{\partial^2 u}{\partial x \partial t}\right)\left(\frac{\partial^2 u}{\partial x \partial t}\right) dt = \left(\frac{\partial}{\partial x}\right)\left(\frac{\partial^2 u}{\partial x \partial t}\right)\delta u(x,t)\Big|_{t_1}^{t_2} - \int_{t_1}^{t_2} \delta u(x,t)\left(\frac{\partial}{\partial x}\right)\left(\frac{\partial^3 u}{\partial x \partial t^2}\right) dt$$

$$\int_{t_1}^{t_2} \delta T dt = \int_0^L \left(\rho A \left(\left(\frac{\partial u}{\partial t}\right)\delta u(x,t)\Big|_{t_1}^{t_2} - \int_{t_1}^{t_2} \delta u(x,t)\left(\frac{\partial^2 u}{\partial t^2}\right) dt \right) + \rho v^2 I_p \left(\left(\frac{\partial}{\partial x}\right)\left(\frac{\partial^2 u}{\partial x \partial t}\right)\delta u(x,t)\Big|_{t_1}^{t_2} - \int_{t_1}^{t_2} \delta u(x,t)\left(\frac{\partial}{\partial x}\right)\left(\frac{\partial^3 u}{\partial x \partial t^2}\right) dt \right) \right) dx$$

$$= -\int_0^L \int_{t_1}^{t_2} \rho A \delta u(x,t)\left(\frac{\partial^2 u}{\partial t^2}\right) dt dx - \int_0^L \int_{t_1}^{t_2} \rho v^2 I_p \delta u(x,t)\left(\frac{\partial}{\partial x}\right)\left(\frac{\partial^3 u}{\partial x \partial t^2}\right) dt dx$$

The last part needs to have another integration by parts, on the x variable.

$$\int_{t_1}^{t_2} \int_0^L \rho v^2 I_p \delta u(x,t)\left(\frac{\partial}{\partial x}\right)\left(\frac{\partial^3 u}{\partial x \partial t^2}\right) dx dt = \int_{t_1}^{t_2} \rho v^2 I_p \left(\frac{\partial^3 u}{\partial x \partial t^2}\delta u(x,t)\Big|_0^L - \int_0^L \delta u(x,t)\left(\frac{\partial}{\partial x}\right)\left(\frac{\partial^3 u}{\partial x \partial t^2}\right) dx \right) dt$$

Thus:

$$\int_{t_1}^{t_2} \delta T dt = -\int_0^L \int_{t_1}^{t_2} \rho A \delta u(x,t)\left(\frac{\partial^2 u}{\partial t^2}\right) dt dx - \int_{t_1}^{t_2} \rho v^2 I_p \left(\frac{\partial^3 u}{\partial x \partial t^2}\delta u(x,t)\Big|_0^L + \int_0^L \delta u(x,t)\left(\frac{\partial}{\partial x}\right)\left(\frac{\partial^3 u}{\partial x \partial t^2}\right) dx \right) dt$$

References

[1] Bergman, R.M., 1968. Asymptotic analysis of some plane problems of the theory of elasticity with couple stresses: PMM vol. 32, n≗ 6, 1968, pp. 1070–1074. *Journal of Applied Mathematics and Mechanics*, *32*(6), pp.1085-1090.

[2] Lim, C.W., Zhang, G. and Reddy, J., 2015. A higher-order nonlocal elasticity and strain gradient theory and its applications in wave propagation. *Journal of the Mechanics and Physics of Solids*, *78*, pp.298-313.Eringen, A.C., 1983. On differential equations of nonlocal elasticity and solutions of screw dislocation and surface waves. *Journal of applied physics*, *54*(9), pp.4703-4710.

[3] Eringen, A.C., 2002. Nonlocal continuum field theories springer, berlin.

[4] Eringen, A.C., 1984. *Theory of nonlocal elasticity and some applications*. Princeton Univ NJ Dept of Civil Engineering.

[5] Lam, D.C., Yang, F., Chong, A.C.M., Wang, J. and Tong, P., 2003. Experiments and theory in strain gradient elasticity. *Journal of the Mechanics and Physics of Solids*, *51*(8), pp.1477-1508.

[6] Fleek, N.A., Muller, G.M., Ashby, M.F. and Hutchinson, J.W., 1994. Strain gradient plasticity: theory and experiments. *Acta Metall Mater*, *42*(3), p.475.

[7] Lei, Y., Adhikari, S. and Friswell, M.I., 2013. Vibration of nonlocal Kelvin–Voigt viscoelastic damped Timoshenko beams. *International Journal of Engineering Science*, *66*, pp.1-13.

[8] Farajpour, A., Ghayesh, M.H. and Farokhi, H., 2018. A review on the mechanics of nanostructures. *International Journal of Engineering Science*, *133*, pp.231-263.

[9] Reddy, J., 2007. Nonlocal theories for bending, buckling and vibration of beams. *International journal of engineering science*, *45*(2-8), pp.288-307.

[10] Thai, H.T., 2012. A nonlocal beam theory for bending, buckling, and vibration of nanobeams. *International Journal of Engineering Science*, *52*, pp.56-64.

[11] Lu, L., Guo, X. and Zhao, J., 2017. A unified nonlocal strain gradient model for nanobeams and the importance of higher order terms. *International Journal of Engineering Science*, *119*, pp.265-277.

[12] Shen, Y., Chen, Y. and Li, L., 2016. Torsion of a functionally graded material. *International Journal of Engineering Science*, *109*, pp.14-28.

[13] Zhu, X. and Li, L., 2017. Twisting statics of functionally graded nanotubes using Eringen's nonlocal integral model. *Composite Structures*, *178*, pp.87-96.

[14] Challamel, N., Zhang, Z., Wang, C.M., Reddy, J.N., Wang, Q., Michelitsch, T. and Collet, B., 2014. On nonconservativeness of Eringen's nonlocal elasticity in beam mechanics: correction from a discrete-based approach. *Archive of Applied Mechanics*, *84*(9), pp.1275-1292.

[15] Fernández-Sáez, J., Zaera, R., Loya, J.A. and Reddy, J., 2016. Bending of Euler–Bernoulli beams using Eringen's integral formulation: a paradox resolved. *International Journal of Engineering Science*, *99*, pp.107-116.

[16] Apuzzo, A., Barretta, R., Luciano, R., de Sciarra, F.M. and Penna, R., 2017. Free vibrations of Bernoulli-Euler nano-beams by the stress-driven nonlocal integral model. *Composites Part B: Engineering*, *123*, pp.105-111.

[17] Wang, Y.B., Zhu, X.W. and Dai, H.H., 2016. Exact solutions for the static bending of Euler-Bernoulli beams using Eringen's two-phase local/nonlocal model. *Aip Advances*, *6*(8), p.085114.

[18] Zhu, X., Wang, Y. and Dai, H.H., 2017. Buckling analysis of Euler–Bernoulli beams using Eringen's two-phase nonlocal model. *International Journal of Engineering Science*, *116*, pp.130-140.

[19] Qing, H., 2022. Well-posedness of two-phase local/nonlocal integral polar models for consistent axisymmetric bending of circular microplates. *Applied Mathematics and Mechanics*, *43*(5), pp.637-652.

[20] Khaniki, H.B., 2018. On vibrations of nanobeam systems. *International Journal of Engineering Science*, *124*, pp.85-103.

[21] Fakher, M. and Hosseini-Hashemi, S., 2020. Vibration of two-phase local/nonlocal Timoshenko nanobeams with an efficient shear-locking-free finite-element model and exact solution. *Engineering with Computers*, pp.1-15.

[22] Shaat, M., Faroughi, S. and Abasiniyan, L., 2017. Paradoxes of differential nonlocal cantilever beams: Reasons and a novel solution. *arXiv preprint arXiv:1802.01494*.

[23] Rao, S.S., 2019. *Vibration of continuous systems*. John Wiley & Sons.

[24] Polyanin, A.D. and Manzhirov, A.V., 2008. *Handbook of integral equations*. Chapman and Hall/CRC.